ELSEVIER

Coordination Chemistry Reviews
174 (1998) 391–416

COORDINATION CHEMISTRY REVIEWS

pH-Dependent metal-based redox couples as models for proton-coupled electron transfer reactions

Spencer J. Slattery [a], Jean K. Blaho [b], Joseph Lehnes [b], Kenneth A. Goldsby [b,*]

[a] *Department of Chemistry, State University of West Georgia, Carrollton, GA 30118, USA*
[b] *Department of Chemistry, Florida State University, Tallahassee, FL 32306-4390, USA*

Received 30 October 1997; received in revised form 8 May 1998; accepted 26 May 1998

Contents

Abstract

An overview of proton-coupled electron transfer in transition metal–ligand systems known to exhibit pH-dependent metal-based redox potentials is presented. The systems of interest can be thought of as MLH_m complexes, where M is a redox-active metal and LH_m is a ligand in the inner-coordination sphere containing at least one ionizable hydrogen. The use of pH-dependent redox potentials to determine proton-coupled electron transfer reactions is described, along with some important factors for designing and studying complexes that exhibit this behavior. This chemistry is illustrated by a survey of the common transition metal–ligand systems known to give pH-dependent redox potentials indicative of proton-coupled electron transfer.

* Corresponding author. Tel: +1 904 644 3204; Fax: +1 904 644 8281; e-mail: goldsby@chem.fsu.edu

0010-8545/98/$ – see front matter
PII S0010-8545(98)00143-X

1. Introduction

1.1. Proton-coupled electron transfer

If electron transfer occurs with a concomitant change in proton content, then the driving force for the electron transfer reaction will depend on the concentration of hydrogen ion; hence, these electron transfer and proton transfer processes are considered to be coupled. Proton-coupled electron transfer (PCET) processes permeate chemical reactivity. For most of us, our introduction to PCET reactions occurred in general chemistry in the form of balancing redox equations in acidic or basic solution. The coupling of electron transfer and proton transfer is readily indicated by the presence of hydrogen ion (or hydroxide ion) in the half reaction, as illustrated in Eqs. (1) and (2) for the common inorganic oxidizing reagents dichromate and perchlorate, respectively:

$$Cr_2O_7^{2-} + 14H^+ + 6e^- \rightarrow 2Cr^{3+} + 7H_2O \quad (1)$$

$$ClO_4^- + 2H^+ + 2e^- \rightarrow ClO_3^- + H_2O \quad (2)$$

One practical consequence of the presence of hydrogen ion in the half reaction is that the potential (and hence the effectiveness of the oxidant) will depend upon the solution pH.

Many organic redox processes also involve changes in proton content [1,2], as illustrated in Eq. (3) for the oxidation of a secondary alcohol to a ketone:

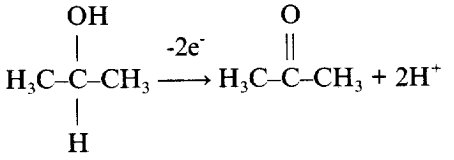

(3)

The two-electron/one-proton oxidation of nicotinamide adenine dinucleotide is but one example of a biologically important reversible PCET reaction [Eq. (4)] [3]:

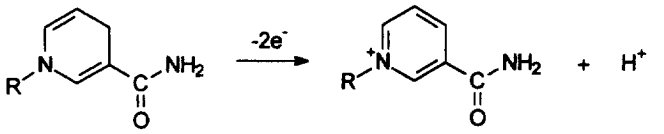

(4)

In fact, PCET reactions are common in nature. Numerous biological processes are known to involve proton-coupled processes, including redox-driven proton pumps in mitochondria [4,5], microbial iron transport [6,7], and the action of molybdenum [8] and manganese [9,10] in enzymatic transformations. In addition, since the aqueous solution chemistry of many elements involves proton-coupled reactions [11], PCET reactions are also known to be important in the sciences of metal corrosion and radioactive waste disposal, as well as in many geological processes [12].

There is a growing interest in developing models for PCET reactions [13]. Given the important role that transition metal complexes have played in the study of electron transfer reactions, it is natural to look to transition metal complexes as

models for the study of PCET. Ideally, one would like to study discrete, reversible one-proton/one-electron processes. Oxidation or reduction of main group compounds generally results in the formation of highly reactive radicals. To obtain stable products, a net transfer of an even number of electrons is required. For example, the oxidation of alcohols to aldehydes and ketones [illustrated in Eq. (3) for the oxidation of isopropanol to acetone] is a two-electron process. Therefore, in order to obtain reversible PCET with main group compounds, it is necessary to transfer electrons in multiples of two. A well-known example of reversible PCET in an organic molecule is the two-electron/two-proton oxidation of hydroquinone [Eq. (5)] [14]:

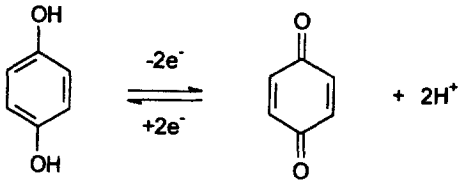

(5)

Biological systems commonly employ two-electron, two-proton redox couples, as with the electron transport chain and oxidative phosphorylation in which electron transfer drives proton transfer against a hydrogen ion concentration gradient to generate ATP from ADP [3,15,16]. Although it is possible to generate relatively stable radicals based on main group compounds [17], these compounds are the exceptions; hence radicals are generally not suited for the study of single electron transfer processes.

In contrast, many transition metal complexes are stable in two or more consecutive oxidation states, making reversible, metal-localized, one-electron redox processes common. The unpaired electrons are localized in d-orbitals, so the paramagnetic species formed can be quite stable. For this reason, there are abundant examples of reversible PCET processes for transition metal compounds. When a ligand containing an ionizable proton is coordinated to a metal ion, the acidity of that ligand generally increases due to stabilization of the conjugate base by the metal cation [18–21]. Since increasing the charge of the cation will usually further stabilize the anionic conjugate base, it follows that the coordinated ligand will become more acidic when the charge of the cation is increased. Therefore, when a ligand containing an ionizable proton is coordinated to a particular metal, the K_a of the complex will increase with the oxidation state of the metal [22]. For example, pK_a^{II} for $Fe(H_2O)_6^{2+}$ is 9.5; oxidation of Fe(II) to Fe(III) gives $pK_a^{III}=2.2$ for $Fe(H_2O)_6^{3+}$ [23]. A metal-localized redox process will show a pH-dependent couple if deprotonation (protonation) of the ligand occurs upon oxidation (reduction) of the complex in the pH range studied and if deprotonation of the ligand affects the metal-localized redox potential. Therefore, the observation of pH-dependent potentials is a powerful tool for recognizing and characterizing proton-coupled redox processes.

The purpose of this paper is to survey the common transition metal complexes which exhibit pH-dependent redox potentials indicative of PCET. It is hoped that this survey will serve as a toolbox for others who wish to model proton-coupled

electron transfer reactions or exploit the pH-dependent redox potentials of these complexes.

1.2. pH-Dependent redox potentials

A general equation for a pH-dependent redox couple is given in Eq. (6), where Ox is the oxidized species and Red is the reduced species:

$$\mathrm{Ox} + n(\mathrm{e}^-) + m(\mathrm{H}^+) \rightleftharpoons \mathrm{Red}(\mathrm{H}^+)_m \tag{6}$$

The measured half-wave potential ($E_{1/2}$) where $[\mathrm{Ox}]=[\mathrm{Red}(\mathrm{H}^+)_m]$ is predicted by the Nernst equation to have a pH dependence according to the following relationship in Eq. (7) [24], where D_o and D_r are the respective diffusion coefficients of the oxidized and reduced species, m is the number of protons, n is the number of electrons, $E^{\circ\prime}$ is the hypothetical formal potential (assumes that the n-electron/m-proton process occurs at pH 0), and $E_{1/2}$ is the measured redox potential:

$$E_{1/2} = E^{\circ\prime} - [0.059/n] \log(D_o/D_r)^{1/2} - 0.059(m/n)\mathrm{pH} \tag{7}$$

The redox potentials (relative to a reference electrode such as the saturated sodium calomel electrode, SSCE) can be determined experimentally using techniques such as cyclic voltammetry [25–28] or differential pulse voltammetry [25,29]. The diffusion coefficients (D_o and D_r) are often assumed to be equal, removing the middle term in Eq. (7).

The dependence of redox potential upon hydrogen ion concentration is conveniently visualized in a pH–potential diagram, commonly referred to as a Pourbaix diagram [11,20–22,30,31] or predominance area diagram. {Strictly speaking, a Pourbaix diagram is a three-dimensional surface, with the three dimensions E, pH, and activity (see ref. [32]). A two-dimensional diagram of E vs. pH is called a predominance diagram, but is also commonly referred to by many authors as a Pourbaix diagram (see ref. [20]).} These diagrams find wide use in many fields, including corrosion science and geochemistry [12,24]. The pH–potential diagrams for simple transition metal ions are typically complex, involving multiple proton and electron transfer processes [11,30,31]. The pH–potential diagram for a one-electron redox process involving a hypothetical $M^{II}LH$ complex containing a single ionizable proton is shown in Fig. 1. {In this treatment we will assume that the metal-localized couple involves the M(III) and M(II) oxidation states; however, this treatment can be generalized to any $M^{(n+1)+/n+}$ couple. Hypothetical redox reactions will generally be written as reductions [e.g. Eq. (6)], however, specific examples will be written as either oxidations [e.g. Eq. (32)] or reductions [e.g. Eq. (42)], depending on the original oxidation state of the complex prior to measurement of the potential. All redox potentials are reported as reduction potentials.} The horizontal line in the acidic pH region represents the pH-independent redox process in which both the oxidized and reduced species are protonated [Eq. (8)]:

$$M^{III}LH + e^- \rightarrow M^{II}LH \tag{8}$$

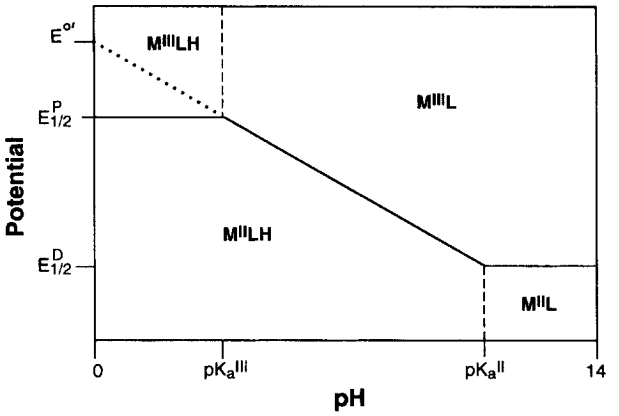

Fig. 1. pH–potential diagram for the hypothetical $M^{II}LH$ complex exhibiting a pH-dependent M(III/II) couple. $E^{\circ\prime}$ is the formal potential of the [M(III)L]/[M(II)LH] couple; $E^{D}_{1/2}$ is the formal potential of the [M(III)L]/[M(II)L] couple; $E^{P}_{1/2}$ is the formal potential of the [M(III)LH]/[M(II)LH] couple. pK_a^{II} and pK_a^{III} are pK_a values of the M(II) and M(III) species, respectively.

the horizontal line in the basic region represents the pH-independent redox process in which both the oxidized and reduced species are deprotonated [Eq. (9)]:

$$M^{III}L + e^- \rightarrow M^{II}L \tag{9}$$

The diagonal line corresponds to the pH-dependent redox process where reduction/oxidation of the metal center is coupled to protonation/deprotonation of the ligand [Eq. (10)]:

$$M^{III}L + e^- + H^+ \rightarrow M^{II}LH \tag{10}$$

The slope of this line is 59 mV/pH unit according to Eq. (7) for a one-electron/one-proton couple. The vertical line in the acidic pH region represents the acid/base equilibrium for the oxidized complex [Eq. (11)]:

$$M^{III}LH \rightleftharpoons H^+ + M^{III}L \tag{11}$$

for which the acid dissociation constant is given by:

$$K_a^{III} = [H^+][M^{III}L]/[M^{III}LH] \tag{12}$$

The horizontal line in the acidic region corresponds to the potential at which $[M^{III}LH] = [M^{II}LH]$, and the diagonal line corresponds to the potential at which $[M^{III}L] = [M^{II}LH]$. At the intersection point, $[M^{III}LH] = [M^{II}LH] = [M^{III}L]$ and Eq. (12) reduces to $K_a^{III} = [H^+]$. Hence $pK_a^{III} = pH$ at the vertical line in the acidic region. By a similar argument, the vertical line in the basic region represents the acid/base equilibrium for the reduced complex [Eqs. (13) and (14)]:

$$M^{II}LH \rightleftharpoons H^+ + M^{II}L \tag{13}$$

$$K_a^{II} = [H^+][M^{II}L]/[M^{II}LH] \tag{14}$$

and $pK_a^{II} = pH$. Note that these results are consistent with Eq. (7) which predicts a slope of $59(m/n)$ mV/pH unit for n-electron/m-proton reaction: a redox reaction that does not involve the transfer of a proton ($m=0$) will be a horizontal line; an acid/base equilibrium that does not involve a redox reaction ($n=0$) will be a vertical line; and a one-electron/one-proton process ($n=1$, $m=1$) will have a slope of 59 mV/pH unit.

1.3. Criteria for useful PCET models

In principle any redox reaction coupled to a rapid change in proton content will give rise to a pH-dependent redox couple as described for the hypothetical $M^{II}LH$ complex. For this complex to be useful for the study and exploitation of PCET, however, certain additional criteria should be met.

1.3.1. One-electron/one-proton couples

The simplest models for proton-coupled electron transfer would be complexes that exhibit a single one-electron/one-proton couple over wide pH and potential ranges. The complex $Ru(bpy)_2Cl_2$ exhibits Ru(III/II) and Ru(IV/III) couples at 0.32 and 1.95 V vs. SSCE in acetonitrile [33,34], respectively; however, the analogous couples for $[(bpy)_2(py)Ru(H_2O)]^{2+}$ occur at 0.42 and 0.53 V in water at pH 7 [18]. The close spacing of the potentials for $[(bpy)_2(py)Ru(H_2O)]^{2+}$ results from the ability of this complex to lose a proton with each electron such that the overall charge of the complex does not change [Eqs. (15) and (16)]:

$$[(bpy)_2(py)Ru^{II}OH_2]^{2+} \rightleftharpoons [(bpy)_2(py)Ru^{III}OH]^{2+} + H^+ + e^- \quad (15)$$

$$[(bpy)_2(py)Ru^{III}OH]^{2+} \rightleftharpoons [(bpy)_2(py)Ru^{IV}O]^{2+} + H^+ + e^- \quad (16)$$

By limiting the inner-coordination sphere to a single ionizable proton, one can eliminate the complications caused by the subsequent ionization of additional protons. The complex $[(tpy)(bpy)Ru^{II}pzH]^{2+}$ exhibits a single pH-dependent Ru(III/II) couple [Eq. (17)]:

$$[(tpy)(bpy)Ru^{II}pzH]^{2+} \rightleftharpoons [(tpy)(bpy)Ru^{III}pz]^{2+} + H^+ + e^- \quad (17)$$

and the Ru(IV/III) couple is not observed out to the oxidative limit of the solvent window [35].

1.3.2. Region of pH-dependent behavior

The pH-dependent region is defined in Fig. 1 by four parameters: $E_{1/2}^{P}$ [the potential for the protonated couple, Eq. (8)], $E_{1/2}^{D}$ [the potential for the deprotonated couple, Eq. (9)], pK_a^{III}, and pK_a^{II}. These parameters can be used to construct the thermodynamic cycle in Fig. 2. In order to observe the full range of pH dependence, it is necessary for the $M^{III}L/M^{II}LH$ couple to fall between the potentials for the oxidation and reduction of water in that pH range. For example, the complex $[Ru(pap)_2(H_2O)_2]^{2+}$ is easily deprotonated ($pK_a^{II} = 6.8$); however, PCET is not observable because the Ru(III/II) couple is too high [36]. For the corresponding

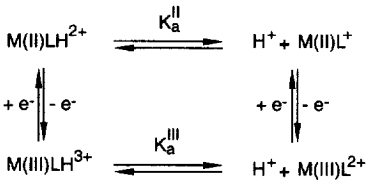

Fig. 2. Thermodynamic cycle for the hypothetical $M^{II}LH$ complex.

polypyridyl complex, the Ru(III/II) couple is well within the solvent window. The above comparison illustrates the influence the spectator ligands can have on the M(III/II) couple; however, one must also consider the simultaneous effect on pK_a^{II} and pK_a^{III}. Complexes containing strong π-acceptors as spectator ligands will remove electron density from the metal, increasing the acidity of the coordinated LH ligand. This can be illustrated by comparing the mono-aqua complexes $[(pap)_2(py)Ru^{II}(OH_2)]^{2+}$ [36], $[(bpy)_2(py)Ru^{II}(OH_2)]^{2+}$ [18], and $[(NH_3)_5Ru^{II}(OH_2)]^{2+}$ [18] which have pK_a values of 6.8, 10.3, and ~13, respectively. Since the pH dependence occurs over the range $pH = pK_a^{III}$ to pK_a^{II}, it is desirable that pK_a^{III} correspond to the acidic region ($pH \geqslant 1$) and/or pK_a^{II} correspond to the basic region ($pH \leqslant 14$). For example, since $[(NH_3)_5Ru^{II}(pyzH)]^{3+}$ has a pK_a^{II} value of 2.5, PCET will be observed only at $pH < 2.5$.

In addition to specifying that the pH-dependent couple must occur within measurable pH and potential ranges, it is also desirable to maximize the window of pH-dependent behavior. From Fig. 1, the pH-dependent redox process will occur over a pH range determined by the difference between pK_a for the oxidized and reduced complexes [Eq. (18)]:

$$\Delta pK_a = pK_a^{III} - pK_a^{II} \tag{18}$$

In other words, for the complex $M^{II}LH$ to exhibit pH-dependent M(III/II) potentials, changing the oxidation state on the metal must significantly affect the acidity of the coordinated ligand. Conversely, deprotonation of the ligand should significantly affect the M(III/II) couple. For a one-electron/one-proton couple, Eq. (7) specifies a 59 mV/pH unit dependence, i.e.

$$\Delta E_{1/2} = (59\ \text{mV})\Delta pK_a \tag{19}$$

where

$$\Delta E_{1/2} = E_{1/2}^{P} - E_{1/2}^{D} \tag{20}$$

So, the extent of interaction between the metal center and the ionizable proton determines the size of the pH-dependent region, and the extent of this interaction is equivalently reflected in ΔpK_a and $\Delta E_{1/2}$. Sigma-bonding (field and inductive effects) [37] and pi-bonding interactions both have an influence.

1.3.3. Sigma-bonding (field and inductive) effects

As mentioned above, increasing the charge of a metal ion tends to enhance the acidity of its coordinated ligands. Although it is difficult to separate inductive (through sigma bonds) and field (through space) effects, the sum of these effects is expected to be proportional to Z/r, where Z is the charge of the ion and r is the ionic radius [37]. If the field effect is the major factor influencing pK_a of the coordinated ligand, then the acidity of the ligand will increase with increasing oxidation state for a particular metal. Furthermore, since field effects decrease with distance ($1/r$), ligands with the site of deprotonation closer to the metal would be expected to be more sensitive to the oxidation state of the metal. Therefore, the acidity of a coordinated ligand will be enhanced to a greater extent which can be measured by the difference between pK_a for the free ligand and pK_a for the coordinated ligand. This relationship can be seen for a series of $[(NH_3)_5Ru^{III}LH]^{3+}$ complexes, where LH is H_2O, pyrazole, or imidazole. The $(NH_3)_5Ru^{III}$ center lowers the pK_a of water by 11.6 units (from 15.7 to 4.1), pyrazole by 8.2 units (from 14.2 to 5.98), and imidazole by 5.3 units (from 14.2 to 8.9) [19].

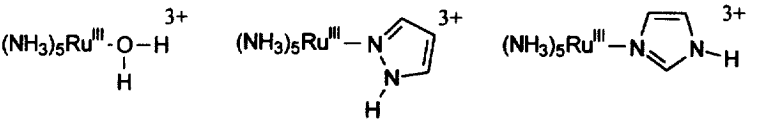

It follows that a larger region of pH dependence (ΔpK_a) will result when the site of deprotonation is closer to the metal.

1.3.4. Pi-bonding effects

Shepherd has demonstrated that for coordination of imidazole to different metals of the same size and overall charge, the d^n configuration of the metal has a large influence on the pK_a of the complex. For example, the d^n configuration had a greater influence than σ induction (and field) effects on the pK_a of coordinated imidazoles, when studied for Cr(III), Fe(III), Co(III), Rh(III), and Ir(III) [38]. This effect was said to be due to the π-donor capability of imidazole; i.e. when coordinated to a metal which has partially empty $d\pi$ orbitals, the acidity of the ligand will be more enhanced. A similar result has been observed for the acidity of cationic aqua acids [20]. The acidity of the coordinated water increased with increasing polarizability and electronegativity of the metal, both factors leading to an increase in the covalency of the M–O bond. For example, for Mg^{2+} $pK_a = 11.42$, but for Hg^{2+} $pK_a = 3.70$ (Mg^{2+} and Hg^{2+} are of comparable size, hence comparable ionic potential). Another revealing example of π-effects is provided by $[(NH_3)_5Ru^{II}(pyz)]^{2+}$. For the Ru(II) complex, pyrazine is actually more basic than the free ligand. The pK_a of the conjugate acid of free pyrazine is 0.6 [Eq. (21)], as compared to 2.5 for the Ru(II) complex [Eq. (22)]:

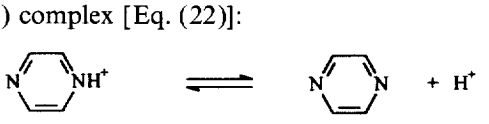

(21)

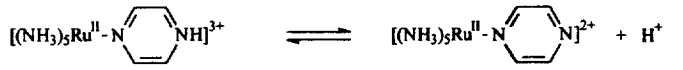

(22)

The enhanced basicity of the pyrizine coordinated to Ru(II) was attributed to π-backdonation into the protonated pyrazine. The protonated pyrazine is a better π-accepter than the unprotonated pyrazine, as indicated by the shift to lower energy of the metal-to-ligand [dπ→π*(pyrazine)] charge transfer band. When the metal is Ru(III), an increase in basicity is not observed [Eq. (23), $pK_a^{III} = -0.8$], since Ru(III) is not a good π-donor [19]:

(23)

This phenomenon is not observed when the pyrazine is replaced by H_2O, where pK_a of the $Ru^{II}OH_2$ complex has been determined to be roughly 12–13, as compared to 15.7 for the uncoordinated water molecule. This result, combined with the fact that good π-acceptor metals such as Ru(III) will enhance the acidity of π-donor ligands relative to metals which are not good π-acceptors [e.g. Ru(II)], suggests another way in which to amplify the difference in pK_a between the two oxidation states. Specifically, it seems probable that the ΔpK_a will be enhanced when the LH ligand can act as a good π-acceptor when coordinated to M(II) and a good π-donor when M(II) is oxidized to M(III).

1.3.5. Chemical and electrochemical reversibility of the couple

If the M(II)LH complexes are to be used to study electron transfer reactions, it is desirable for them to be stable in both oxidation states. Electrochemically, this stability is reflected in the chemical reversibility of the redox couple. To ensure chemical reversibility, the model complex should be substitutionally inert in both oxidation states. The wide use of ruthenium polypyridyl complexes to study electron transfer reactions is due in part to their thermodynamic stability. Studies of first-row transition metal complexes are made easier by the use of multidentate ligands to occupy all coordination sites. A saturated coordination sphere is also necessary in order to avoid secondary pH dependence due to aqua ligands. In order to measure redox potentials, complexes should be water soluble at all pHs and in both oxidation states. In some cases, the use of mixed solvents, such as acetonitrile/water [39,40] or dioxane/water [41] offer effective solutions to this problem.

Finally, electrochemical reversibility must be considered. A chemically reversible electron transfer can lead to an irreversible electrode response, as indicated by large peak-to-peak splitting (ΔE_p) in cyclic voltammetry and/or unequal peak current ratios in cyclic voltammetry and differential pulse polarography. This condition is termed electrochemical irreversibility and is caused by slow heterogeneous electron transfer kinetics between the surface of the electrode and the chemical reactant [36]. Heterogeneous electron transfer rates are sensitive to the electrode surface, which is in turn sensitive to the preparation of the electrode by techniques such as polishing or chemical or electrochemical pretreatment. In general, carbon is the electrode of

choice for electrochemical measurements in water, and carbon electrodes are particularly susceptible to surface effects. A variety of electrode materials, such as glassy carbon, pyrolytic graphite, and carbon paste, are available, and these surfaces are very sensitive to pretreatment procedures [42,43]. Oxidative activation of a glassy carbon electrode has been shown to significantly enhance the electrode response for ruthenium–aqua/hydroxo/oxo couples, some other positively charged ions, and some organic processes (e.g. *o*-quinone/hydroquinone). It is likely that oxidative activation creates functionalities on the carbon surface (e.g. phenolic and carboxylic groups) which facilitate the heterogeneous electron transfer reaction. Changes in the electrode–solution interface result in modification of the heterogeneous electron transfer rate, which affects the reversibility of the couple.

One must also consider the role of electrostatics to understand the type of response that a molecule gives at an activated surface. The Fe(III/II) couple involving the negatively charged complexes $[Fe(CN)_6]^{3-}$ and $[Fe(CN)_6]^{4-}$ gave improved reversibility at a glassy carbon electrode activated by chemical reduction, when the pH was altered from pH 8 to pH 3. For the positively charged complex, $[Ru(NH_3)_6]^{3+}$, the reversibility of the Ru(III/II) couple at this surface was decreased when the pH was changed from pH 8 to pH 3 [44]. This difference in the behavior of the oppositely charged complexes has been attributed to the different affinities for ions of various charge to the surface present at the two pH values. When the pH is changed from 8 to 3, the groups at the surface of the carbon electrode (e.g. carbonyl groups) are protonated, which tends to attract negative ions and repel positive ions. Hence, the reversibility of the $[Fe(CN)_6]^{3-/4-}$ couple is increased while the reversibility of the $[Ru(NH_3)_6]^{3+/2+}$ couple is decreased. Behavior at the electrode is important since electrochemical measurements play an important role in the study of PCET reactions.

2. Metal–ligand systems giving pH-dependent redox potentials

The remainder of this paper surveys the common metal–ligand systems known to give pH-dependent redox potentials due to PCET. Each of these systems can be thought of as a MLH_m complex, where M is a redox active metal and LH_m is a ligand in the inner-coordination sphere containing at least one ionizable hydrogen.

2.1. Aqua/hydroxo/oxo complexes

Metal–aqua complexes can undergo pH-dependent redox reactions by virtue of the deprotonation of the coordinated water as illustrated in Eqs. (24) and (25) for sequential one-electron/one-proton couples:

$$[M^{n+}OH_2]^{n+} \rightleftharpoons [M^{(n+1)+}OH]^{n+} + H^+ + e^- \quad (24)$$

$$[M^{(n+1)}OH]^{n+} \rightleftharpoons [M^{(n+2)+}{=}O]^{n+} + H^+ + e^- \quad (25)$$

For this reason, transition metal ions generally exhibit pH-dependent redox poten-

tials. Furthermore, because loss of the electron is coupled to loss of a proton in each of the above steps, the overall charge of the complex does not change, and multiple redox couples can occur within a narrow potential range. For metal ions containing multiple aqua ligands, the redox behavior can be quite complex. When multiple electron transfers and multiple acid/base reactions occur, the resulting pH–potential diagrams become complicated, as seen in Fig. 3 for aqueous chromium [32]. The chromium system is complex because there are several accessible oxidation states [Eqs. (26)–(28)], and several acid/base processes [Eqs. (29)–(31)]. Furthermore, the acid/base reactions (indicated by vertical lines) are more than just simple proton transfers. At some boundaries, crossing the vertical line results in a change in the inner-coordination sphere, including the formation of oligomers [Eqs. (29) and (30)] and precipitation of solid $Cr(OH)_3$ [Eq. (31)]. In other systems, even higher order oligomers can be formed [45]:

$$Cr^{3+} + e^- \rightleftharpoons Cr^{2+} \tag{26}$$

$$[Cr^{IV}O_4]^{4-} + 4H^+ + e^- \rightleftharpoons [Cr^{III}(OH)_4]^- \tag{27}$$

$$[Cr^{V}O_4]^{3-} + 4H^+ + 2e^- \rightleftharpoons [Cr^{III}(OH)_4]^- \tag{28}$$

$$3Cr^{3+} + 4OH^- \rightleftharpoons [Cr_3(OH)_4]^{5+} \tag{29}$$

$$[Cr_2O_7]^{2-} + H_2O \rightleftharpoons 2[CrO_4]^{2-} + 2H^+ \tag{30}$$

$$[Cr(OH)_4]^- \rightleftharpoons Cr(OH)_3(s) + OH^- \tag{31}$$

The situation is considerably simplified by limiting the number of water molecules in the inner-coordination sphere. The aqueous electrochemistry of *cis*- and *trans*-$[(bpy)_2M^{II}(OH_2)_2]^{2+}$ (M = Ru, Os) has been reported by Meyer and coworkers [46,47]. The resulting pH–potential diagrams are shown in Fig. 4. Since subsequent oxidations are not subjected to systematically increasing electrostatic barriers, four successive one-electron/one-proton couples are observed at pH 4, leading to the

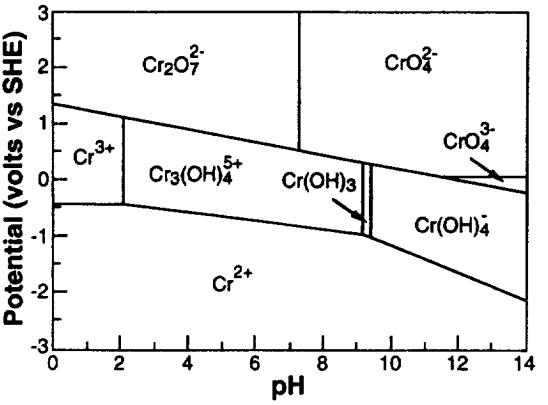

Fig. 3. pH–potential diagram for chromium (adapted from ref. [32]).

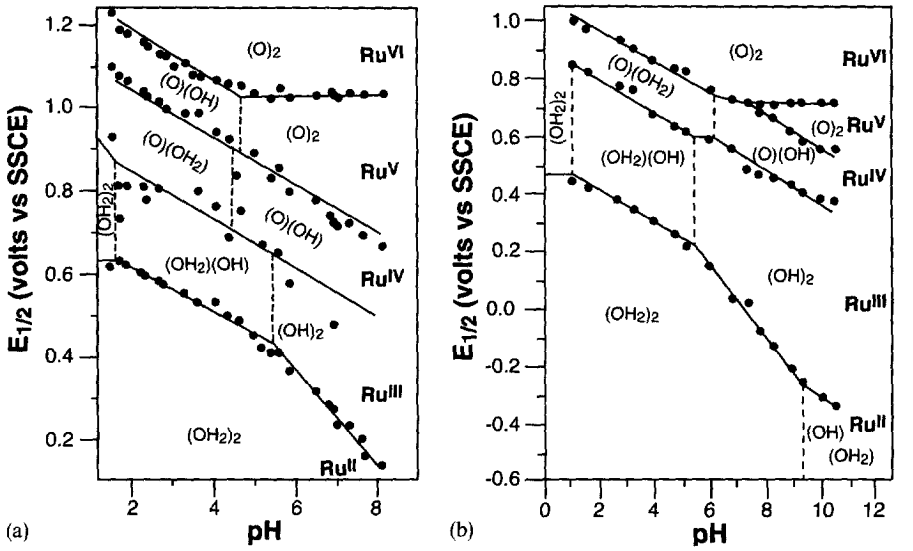

Fig. 4. pH–potential diagram for (A) *cis*-$[(bpy)_2Ru^{II}(OH_2)_2]^{2+}$ and (B) *trans*-$[(bpy)_2Ru^{II}(OH_2)_2]^{2+}$ (adapted from ref. [47]).

formation of $[(bpy)_2M^{VI}(O)_2]^{2+}$ [Eqs. (32)–(35)]:

$$[(bpy)_2M^{II}(OH_2)_2]^{2+} \rightleftharpoons [(bpy)_2M^{III}(OH)(OH_2)]^{2+} + H^+ + e^- \quad (32)$$

$$[(bpy)_2M^{III}(OH)(OH_2)]^{2+} \rightleftharpoons [(bpy)_2M^{IV}(OH)_2]^{2+} + H^+ + e^- \quad (33)$$

$$[(bpy)_2M^{IV}(OH)_2]^{2+} \rightleftharpoons [(bpy)_2M^{V}(OH)(O)]^{2+} + H^+ + e^- \quad (34)$$

$$[(bpy)_2M^{V}(OH)(O)]^{2+} \rightleftharpoons [(bpy)_2M^{VI}(O)_2]^{2+} + H^+ + e^- \quad (35)$$

The loss of four protons from the two coordinated water molecules permits five oxidation states to be accessible within a potential range of only 500 mV!

The number of PCET reactions can be further reduced by limiting the inner-coordination sphere to one aqua ligand; however, multiple redox reactions can still occur within a narrow potential range due to sequential deprotonations of the aqua ligand. Recall that at pH 7 the mono-aqua complex $[(bpy)_2(py)Ru^{II}(OH_2)]^{2+}$ exhibits two closely spaced one-electron couples at 0.42 and 0.53 V vs. SCE [Eqs. (15) and (16), respectively] [18,48]. Again, since the overall charge of the complex does not increase, the stepwise increase in the electrostatic barrier normally encountered with sequential oxidations is alleviated by the loss of the protons, thereby rendering the Ru(III/II) and Ru(IV/III) couples within only 110 mV of each other. It is difficult to isolate a single redox species when the redox potentials are closely spaced. For example, the oxidation of Ru(II) by one equivalent of electrons in the present case gives rise to a mixture of oxidation states (9.5% Ru^{II}, 81% Ru^{III} and 9.5% Ru^{IV}). Furthermore, the aqua ligand is considered to be relatively labile which can create complications when studying the electron transfer process.

The analogous mono-aqua complexes $[(tpy)(bpy)M^{II}(OH_2)]^{2+}$ (M = Ru, Os, tpy = 2,2′;6,2″-terpyridine) have also been studied, and a pH–potential diagram for $[(tpy)(bpy)Ru^{II}(OH_2)]^{2+}$ is shown in Fig. 5 [49]. As with the $[(bpy)_2(py)Ru^{II}(OH_2)]^{2+}$ complex, three distinct modes of PCET are observed depending on the solution pH. At neutral pH, the ruthenium complex undergoes a series of one-electron/one-proton couples [Eqs. (36) and (37)]:

$$[(tpy)(bpy)M^{II}(OH_2)]^{2+} \rightleftharpoons [(tpy)(bpy)M^{III}(OH)]^{2+} + H^+ + e^- \quad (36)$$

$$[(tpy)(bpy)M^{III}(OH)]^{2+} \rightleftharpoons [(tpy)(bpy)M^{IV}(O)]^{2+} + H^+ + e^- \quad (37)$$

In highly acidic solution (pH < 1.5), the Ru(III/II) couple becomes pH-independent because Ru(III) remains protonated (H_2O) at this pH [Eq. (38)]. The Ru(IV/III) couple is a one-electron/two-proton process, resulting in the Ru(IV)-oxo species, even at this low pH [Eq. (39)]:

$$[(tpy)(bpy)M^{II}(OH_2)]^{2+} \rightleftharpoons [(tpy)(bpy)M^{III}(OH_2)]^{3+} + e^- \quad (38)$$

$$[(tpy)(bpy)M^{III}(OH_2)]^{3+} \rightleftharpoons [(tpy)(bpy)M^{IV}(O)]^{2+} + 2H^+ + e^- \quad (39)$$

At pH greater than 10, the Ru(II) complex exists as the hydroxo species, and so the Ru(III/II) couple is pH-independent [Eq. (40)]; the Ru(IV/III) couple is still a one-electron/one-proton process [Eq. (37)]:

$$[(tpy)(bpy)M^{II}(OH)]^{+} \rightleftharpoons [(tpy)(bpy)M^{III}(OH)]^{2+} + e^- \quad (40)$$

At very high pH (> 11.5), a two-electron/one-proton process is observed, corresponding to the Ru(IV/II) couple [Eq. (41)]:

$$[(tpy)(bpy)M^{II}(OH)]^{+} \rightleftharpoons [(tpy)(bpy)M^{IV}(O)]^{2+} + H^+ + 2e^- \quad (41)$$

Results for osmium are qualitatively similar, except that a pH-independent Os(V/IV) couple is also observable in the pH range studied.

Aqueous cyclic voltammetry of a related mono-aqua complex,

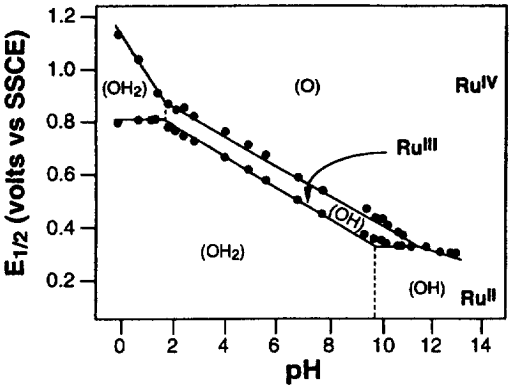

Fig. 5. pH–potential diagram for $[(trpy)(bpy)Ru^{II}(OH_2)]^{2+}$ (adapted from ref. [49]).

$[(tpy)(tmen)Ru^{II}(OH_2)]^{2+}$, has also been studied [50]. In the pH range 1–7, $[(tpy)(tmen)Ru^{II}(OH_2)]^{2+}$ undergoes two sequential one-electron/one-proton oxidations, similar to that of $[(tpy)(bpy)Ru^{II}(OH_2)]^{2+}$, but with potentials lying about 80 mV lower due to the better sigma donor strength of the tmen ligand and its inability to act as a π-acceptor. PCET has also been observed in the analogous complexes $[(tpm)(bpy)Ru(OH_2)]^{2+}$ [51], *cis*- and *trans*-$[(trpy)(pic)Ru(OH_2)]^{+}$ [51], $[(bpy)_2(PR_3)Ru(OH_2)]^{2+}$ [52,53], and $[(edta)Ru(OH_2)]^{-}$ [54]. The macrocyclic complex *trans*-$[(14TMC)Ru^{IV}(O)(OH_2)]^{2+}$ [55] undergoes a reversible two-electron/two-proton Ru(VI/IV) couple in the pH range 1–7, at potentials roughly 300 mV lower than *trans*-$[(bpy)_2Ru^{IV}(O)(OH_2)]^{2+}$. At pH greater than 7, two couples emerge: one corresponding to a pH-independent Ru(VI/V) couple and one corresponding to a one-electron/one-proton Ru(V/IV) couple.

2.2. *Hydroxo/oxo-bridged complexes*

A variety of oxo-bridged bimetallic complexes have been reported which exhibit PCET resulting from protonation of the oxo-bridge. Motivation for studying oxo-bridged manganese systems has stemmed in part from proposed mechanisms for the oxidation of water in photosystem II (PS II) involving a tetramanganese oxo cluster [9,10,56–58]. For example, mixed-valence manganese oxo-bridged complexes such as $[(NN)_2Mn^{III}(O)_2Mn^{IV}(NN)_2]^{3+}$, where NN represents bpy or phen, have been shown to exhibit a one-electron/one-proton couple involving the Mn_2^{III} complex with a bridging oxo and bridging hydroxo [Eq. (42)] [9,10,56,57]:

$$[(NN)_2Mn^{III}(O)_2Mn^{IV}(NN)_2]^{3+} + H^+ + e^- \rightleftharpoons [(L)_2Mn^{III}(O)(OH)Mn^{III}(L)_2]^{3+} \quad (42)$$

A second reversible one-electron/one-proton couple was reported for the phen complex [Eq. (43)]:

$$[(phen)_2Mn^{III}(O)(OH)Mn^{III}(phen)_2]^{3+} + H^+ + e^- \rightleftharpoons [(phen)_2Mn^{III}(OH)_2Mn^{II}(phen)_2]^{3+} \quad (43)$$

Both of these couples can be seen in the pH–potential diagram in Fig. 6 [57]. The mixed-valence complex $[(edda)Mn^{III}(O)_2Mn^{IV}(edda)]^{-}$ also exhibits a one-electron/one-proton $Mn^{III}(O)_2Mn^{IV}/Mn^{III}(O)(OH)Mn^{III}$ couple; however, $[(bispicen)_2Mn^{III}(O)_2Mn^{IV}(bispicen)_2]^{3+}$ does not [56]. Rather, the irreversible cyclic voltammograms observed for this complex have been ascribed to a mechanism involving a one-electron reduction, followed by protonation of one of the bridging oxo groups in a separate step. The differences in reactivity between the various $Mn^{III}(O)_2Mn^{IV}$ complexes have been attributed, in part, to the basicity of the bridging oxo groups [10]. Complications due to decomposition of both reactant and product are seen with these complexes, and the reductions must be carried out in the presence of excess ligand acting as the buffer. The dinuclear complexes are not stable with respect to ligand substitution in coordinating phosphate buffers. In addition, in the

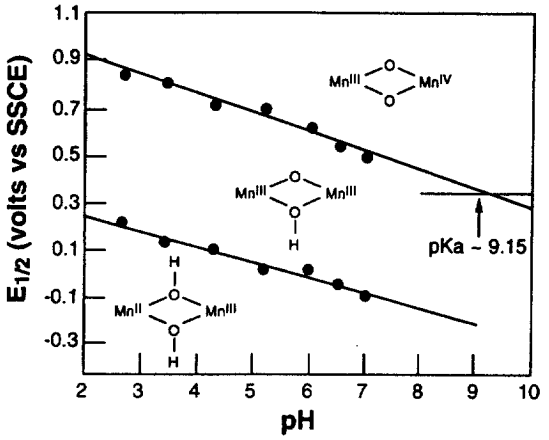

Fig. 6. pH–potential diagram for $[(phen)_2Mn^{III}(O)_2Mn^{IV}(phen)_2](ClO_4)_3$ in 0.1 M phosphate buffer (adapted from ref. [57]).

case of the edda complex, the $Mn^{III}(O)_2Mn^{III}$ product is unstable with respect to dissociation at the bridging oxygen to give two monometallic species.

Cyclic voltammograms of the tri-oxo-bridged complex $[L'Mn^{IV}(O)_3Mn^{IV}L']^{2+}$ (L′ is 1,4,7-trimethyl-1,4,7-triazacyclononane) show a pH-dependent irreversible wave which has been attributed to protonation of one of the bridging oxygens upon reduction to give the $Mn^{III}(O)_2(OH)Mn^{IV}$ complex; however, the pH dependence (155 mV/pH unit) greatly exceeds the 59 mV/pH unit expected for a one-electron/one-proton couple [58]. The irreversibility of the $Mn^{IV}(O)_3Mn^{IV}$/$Mn^{III}(O)_2(OH)Mn^{IV}$ couple was offered as a plausible explanation for this discrepancy, which illustrates the importance of redox reversibility in choosing (or designing) models for PCET reactions.

The oxo-bridged complex, $[((tpy)(pic)Ru^{III})_2O]^{2+}$, undergoes a two-electron, one-proton reversible reduction to form the $Ru^{II}Ru^{II}$ ion consistent with the observed pH dependence of 29 mV/pH unit in the pH range 2–10 [Eq. (44)] [51]:

$$[(tpy)(pic)Ru^{III}(O)Ru^{III}(pic)(tpy)]^{2+} + 2e^- + H^+ \rightleftharpoons [(tpy)(pic)Ru^{II}(OH)Ru^{II}(pic)(tpy)]^+ \quad (44)$$

The complex $[(bpy)_2(OH_2)Ru^{III}(O)Ru^{III}(bpy)_2(OH_2)]^{4+}$ exhibits multiple pH-dependent redox couples indicative of PCET; however, this behavior has been attributed to the two aqua ligands rather than the oxo-bridge [59]. The PCET reactions of $[(edta)Ru^{III}(OH_2)]^-$ may involve the formation of oxo-bridged complexes [54].

2.3. Amine complexes

Metal–amine systems undergo two general types of PCET processes. In the first type, the metal center is oxidized while the amine loses one or more protons

analogous to the metal–aqua systems described in the previous section. Generalized reactions based on one-electron/one-proton reaction steps are shown in Eqs. (45)–(47):

$$[M^{n+}NH_3]^{n+} \rightleftharpoons [M^{(n+1)+}NH_2]^{n+} + H^+ + e^- \quad (45)$$

$$[M^{(n+1)+}NH_2]^{n+} \rightleftharpoons [M^{(n+2)+}{=}NH]^{n+} + H^+ + e^- \quad (46)$$

$$[M^{(n+2)+}{=}NH]^{n+} \rightleftharpoons [M^{(n+3)+}{\equiv}N]^{n+} + H^+ + e^- \quad (47)$$

A second type of PCET involves a ligand-localized redox process driven by the formation of a metal–imine linkage which is stabilized by π-bonding to the low-valent metal [60]:

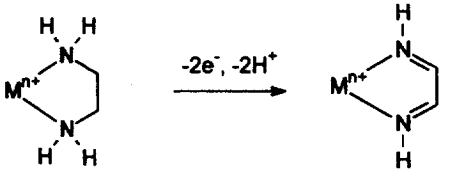

(48)

These systems do not meet the criteria established earlier in this survey (metal-localized redox processes) and will not be considered further.

Given the prominence of reversible PCET in the redox reactions of metal–aqua complexes, the possibility of finding reversible PCET reactions based on metal–amine complexes seems reasonable [Eqs. (45)–(47)]. In both of these systems, deprotonation occurs at an atom directly coordinated to the metal, so the influence on the metal-based redox potential should be substantial. Surprisingly, electrochemically well-characterized examples of reversible PCET reactions based on metal–amine complexes are rare.

The complex $[Cl_2Os^{III}(NH_2CMe_2CMe_2NH_2)_2]^+$ exhibits a reversible Os(IV/III) couple which has been attributed to PCET involving the diamino ligand, as indicated in Fig. 7 [61]. This couple is pH-dependent over the pH range 1–5 with a slope of 60 mV/pH unit, consistent with a one-electron/one-proton process. In contrast, *trans*-$[Cl_2Os^{III}(NH_3)_4]^+$ does not display pH-dependent potentials indicative of

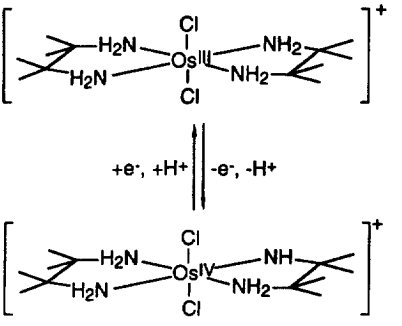

Fig. 7. Reaction scheme for PCET in *trans*-$[(Cl)_2Os^{III}(NH_2CMe_2CMe_2NH_2)_2]^+$ (adapted from ref. [61]).

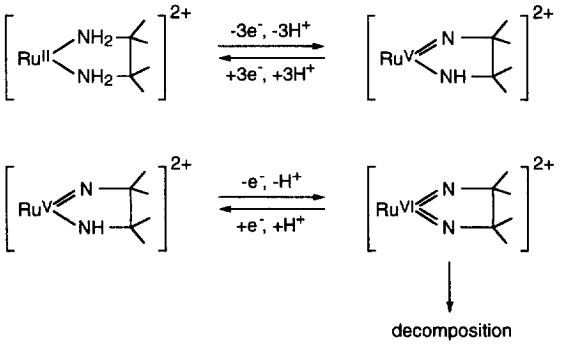

Fig. 8. Reaction scheme for PCET in $[(bpy)_2Ru^{II}(NH_2CMe_2CMe_2NH_2)]^{2+}$ (adapted from ref. [62]).

PCET. The authors suggest that the 2,3-diamino-2,3-dimethylbutane ligand stabilizes high-valent metal complexes relative to simple amine ligands, and postulate that this is due to the chelate effect or better π-donation. No attempt was made to account for the pH dependence on the basis of pK_a values for the coordinated ligands.

A Ru(II) complex based on the 2,3-diamino-2,3-dimethylbutane ligand has also been investigated [62]. The complex $[(bpy)_2Ru(NH_2CMe_2CMe_2NH_2)]^{2+}$ undergoes a reversible three-electron/three-proton oxidation, followed by an irreversible one-electron/one-proton oxidation as shown in Fig. 8. The reversible couple shifts cathodically by $\sim$60 mV/pH unit over the pH range 1–3, as does the irreversible peak potential from pH 1 to 2, both of which are consistent with redox couples involving equal numbers of protons and electrons. Constant-potential electrolysis of the complex permitted isolation of the decomposition product formed by the irreversible oxidation.

The Ru(III/II) couple for the complex $[Ru(sar)_2]^{2+}$ (Fig. 9) is pH-independent at pH<2 [Eq. (49)], but becomes pH-dependent over the pH range 2.5 to 12 [63]:

$$[Ru^{II}(sar)_2]^{2+} \rightleftharpoons [Ru^{III}(sar)_2]^{3+} + e^- \quad (49)$$

The pH dependence indicates a PCET process involving equal numbers of protons and electrons. The magnitude of the current roughly doubles in going from the

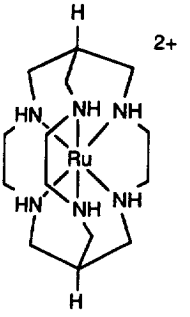

Fig. 9. Structure of the $Ru(sar)^{2+}$ complex (adapted from ref. [63]).

pH-independent to the pH-dependent region, suggesting a switch from a one-electron to a two-electron/two-proton process above pH 3 [Eq. (50)]:

$$[Ru^{II}(sar)_2]^{2+} \rightleftharpoons [Ru^{IV}(sar(-2H^+))_2]^{2+} + 2H^+ + 2e^- \quad (50)$$

2.4. N-Heterocycle complexes

Deprotonation of pyrazoles, imidazoles, and triazoles coordinated to Ru(II) polypyridyl complexes has been shown to result in large shifts in $E_{1/2}$ between the protonated and deprotonated species in acetonitrile and aqueous solvent mixtures [64–68]. For example, the Ru(III/II) couples for the bis-pyrazole complexes *cis*-$[(bpy)_2Ru(pzH)_2]^{2+}$, *cis*-$[(bpy)_2Ru(pzH)(pz)]^+$, and *cis*-$[(bpy)_2Ru(pz)_2]$ occur at 1.18 V, 0.69 V, and 0.30 V, respectively vs. SSCE in acetonitrile [67]. Lack of water solubility of the fully deprotonated complexes prevented electrochemical characterization in purely aqueous solutions.

Haga has extensively investigated the redox reactions of $[(bpy)_2M^{II}(bibzimH_2)]^{2+}$ [40] (M=Ru, Os) in acetonitrile and 1:1 mixture of acetonitrile/water over the pH range 0 to 11. In acetonitrile, the Ru(III/II) couple of the fully protonated complex is 1.12 V vs. SCE, while the Ru(III/II) couple of the fully deprotonated complex is 0.43 V. In 1:1 acetonitrile/water, the M(III/II) couple is reversible at all pHs. Reminiscent of the Ru(II)–aqua complexes, the M(IV/III) couple can be observed in 1:1 acetonitrile/water since deprotonation of the M(III) complex lowers the potential for the second oxidation. The M(IV/III) couple is irreversible; however, it becomes reversible at fast scan rates (5 V/s).

The pH–potential diagram for $[(bpy)_2Ru^{II}(bibzimH_2)]^{2+}$ obtained from these data (Fig. 10) is very similar to the pH–potential diagrams for Ru(II) mono-aqua complexes (Fig. 5) which is understandable given that both complexes contain two ionizable protons. At pH < 0.6, the complex is fully protonated in both the Ru(II) and Ru(III) oxidation states, and the Ru(III/II) couple is pH-independent [Eq. (51)]:

$$[(bpy)_2Ru^{II}(bibzimH_2)]^{2+} \rightleftharpoons [(bpy)_2Ru^{III}(bibzimH_2)]^{3+} + e^- \quad (51)$$

At pH > 10.4, the complex is fully deprotonated in both the Ru(II) and Ru(III) oxidation states, and again the Ru(III/II) couple is pH-independent [Eq. (52)]:

$$[(bpy)_2Ru^{II}(bibzim)] \rightleftharpoons [(bpy)_2Ru^{III}(bibzim)]^+ + e^- \quad (52)$$

In the range pH 0.6 to ~5, the Ru(III/II) couple is pH-dependent (53 mV/pH unit), indicating a one-electron/one-proton process [Eq. (53)]:

$$[(bpy)_2Ru^{II}(bibzimH_2)]^{2+} \rightleftharpoons [(bpy)_2Ru^{III}(bibzimH)]^{2+} + H^+ + e^- \quad (53)$$

At pH ≈7–10, the pH-dependent (53 mV/pH unit) reaction becomes [Eq. (54)]:

$$[(bpy)_2Ru^{II}(bibzbmH)]^+ \rightleftharpoons [(bpy)_2Ru^{III}(bibzim)]^+ + H^+ + e^- \quad (54)$$

For the Ru^{III}/Ru^{IV} couple, the following processes are observed.

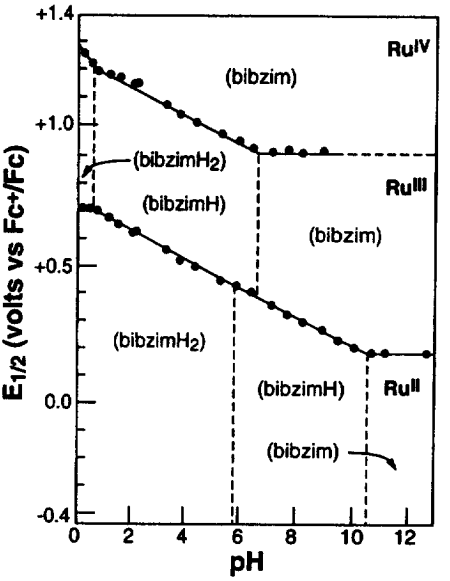

Fig. 10. pH–potential diagram for $[(bpy)_2Ru^{II}(bibzImH_2)]^{2+}$ in CH_3CN/buffer (1:1 v/v) (adapted from ref. [40]).

pH > 7 (pH-independent):

$$[(bpy)_2Ru^{III}(bibzim)]^{+} \rightleftharpoons [(bpy)_2Ru^{IV}(bibzim)]^{2+} + e^{-} \quad (55)$$

pH = 0.5–6 (52 mV/pH unit):

$$[(bpy)_2Ru^{III}(bibzimH)]^{2+} \rightleftharpoons [(bpy)_2Ru^{IV}(bibzim)]^{2+} + H^{+} + e^{-} \quad (56)$$

pH < 0.5 (124 mV/pH unit, indicating a one-electron/two-proton couple):

$$[(bpy)_2Ru^{III}(bibzimH_2)]^{2+} \rightleftharpoons [(bpy)_2Ru^{IV}(bibzim)]^{3+} + 2H^{+} + e^{-} \quad (57)$$

The pH–potential diagram for the complex $[Ru^{II}(py(bzimH)_2)_2]^{2+}$, where $py(bzimH)_2$ is 2,6-bis(benzimidazol-2-yl)pyridine, is similar to that of $[(bpy)_2Ru^{III}(bibzimH_2)]^{2+}$; however, the PCET reactivity is more complex due to the availability of four ionizable hydrogens [68].

As observed for the metal–aqua/hydroxo/oxo complexes, the situation is simplified by reducing the number of ionizable hydrogens on the *N*-heterocycle ligands. The complex $[(tpy)(bpy)Ru(bzimH)]^{2+}$ exhibits a single redox couple within the solvent window (Fig. 11) and the PCET processes are limited to a pH-independent Ru(III/II) couple below pH 5 [Eq. (58)] and a one-proton/one-electron couple above pH 5 [Eq. (59)] [69]:

$$[(tpy)(bpy)Ru^{II}(bzimH)]^{2+} \rightleftharpoons [(tpy)(bpy)Ru^{III}(bzimH)]^{3+} + e^{-} \quad (58)$$

$$[(tpy)(bpy)Ru^{II}(bzimH)]^{2+} \rightleftharpoons [(tpy)(bpy)Ru^{III}(bzim)]^{2+} + H^{+} + e^{-} \quad (59)$$

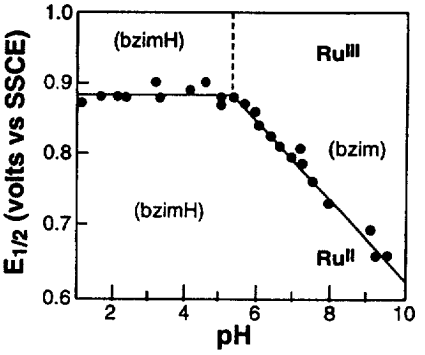

Fig. 11. pH–potential diagram for $[(tpy)(bpy)Ru(bzimH)]^{2+}$ (adapted from ref. [69]).

Note that the pH-independent couple expected at high pH [Eq. (60)] is not observed for $[(tpy)(bpy)Ru(bzimH)]^{2+}$:

$$[(tpy)(bpy)Ru^{II}(bzim)]^{+} \rightleftharpoons [(tpy)(bpy)Ru^{III}(bzim)]^{2+} + e^{-} \quad (60)$$

Apparently the Ru(III/II) couple is too high and the pK_a^{II} is too large for the $[(tpy)(bpy)Ru^{III/II}(bzim)]^{2+/+}$ couple to be observed within the solvent window. Replacing benzimidazole with the more acidic analog benzotriazole (pK_a values for the free ligands are 12 and 8.2, respectively) shifts the pH-independent $[(tpy)(bpy)Ru^{III/II}(bztrz)]^{2+/+}$ couple to within the solvent window (Fig. 12) [69].

2.5. Metal–oxime complexes

Oxime–metal complexes may undergo PCET as indicated below [Eq. (61)]:

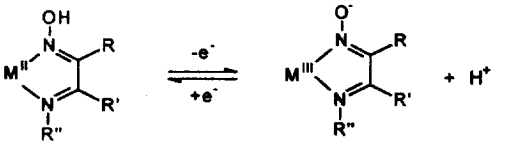

(61)

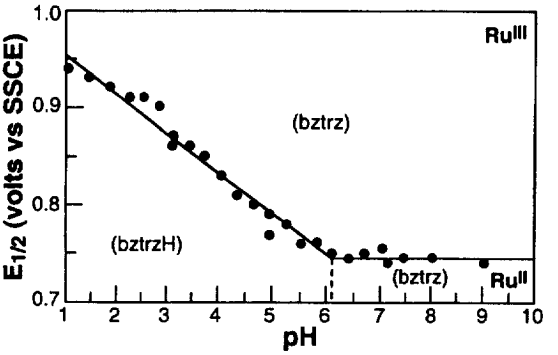

Fig. 12. pH–potential diagram for $[(tpy)(bpy)Ru(bztrzH)]^{2+}$ (adapted from ref. [69]).

Chakravorty has investigated the PCET reactions of nickel(II) and iron(II) oxime complexes, and because these first-row transition metals are substitutionally labile (relative to second- and third-row complexes), studies have tended to employ multidentate ligands [70–74]. The majority of this work has focused on the complex $[Ni(RR'LH_2)]^{2+}$ shown in Fig. 13 [70–72]. The linear hexadentate ligand contains two oxime groups, giving the Ni(II) complex two ionizable protons with pK_as of 5.9 and 7.8. The complex $[Ni(Me_2LH_2)]^{2+}$ is representative of this family. At pH < 5, a single reversible wave is observed by cyclic voltammetry which has been interpreted as a two-electron/two-proton Ni(VI/II) couple based on peak-to-peak splitting of the wave ($\Delta E_p = 30$–40 mV) and constant-potential coulometry [Eq. (62)]:

$$[Ni^{II}(Me_2LH_2)]^{2+} \rightleftharpoons [Ni^{IV}(Me_2L)]^{2+} + 2H^+ + 2e^- \quad (62)$$

As the pH is increased beyond 5, ΔE_p increases, and by pH 6 two distinct couples are observed. The first couple is pH-dependent up to pH 8.5, and the second couple is pH-independent, consistent with Eqs. (63) and (64), respectively:

$$[Ni^{II}(Me_2LH_2)]^{2+} \rightleftharpoons [Ni^{III}(Me_2L)]^{+} + 2H^+ + e^- \quad (63)$$

$$[Ni^{III}(Me_2L)]^{+} \rightleftharpoons [Ni^{IV}(Me_2L)]^{2+} + e^- \quad (64)$$

Above pH 8.5 the first couple also becomes pH-independent [Eq. (65)] due to deprotonation of the Ni(II) complex at that pH:

$$[Ni^{II}(Me_2L)] \rightleftharpoons [Ni^{III}(Me_2L)]^{+} + e^- \quad (65)$$

Comparable results are obtained for $[Ni^{II}(Me_2TH)_2]^{2+}$, where Me_2TH is the tridentate mono-oxime analog of Me_2LH_2 and the pH-dependent regions are determined by the pK_a values for the Ni(II) complex (7.0 and 10.0).

The PCET behavior is simplified for the iron(II) complexes since the iron(IV) state is not accessible; however, the presence of two ionizable protons leads to different mechanisms in different pH regions [73]. For $[Fe^{II}(Me_2LH_2)]^{2+}$, the pK_as of the ionizable protons on the oxime ligands are 4.75 and 7.45. At pH < 4.1, the reversible one-electron/two-proton pH-dependent couple (120 mV/pH unit) is

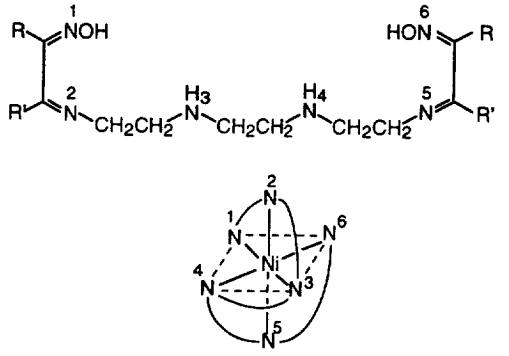

Fig. 13. Structure of Me_2LH_2 and its Ni(II) complex (adapted from ref. [70]).

observed [Eq. (66)]:

$$[Fe^{II}(Me_2LH_2)]^{2+} \rightleftharpoons [Fe^{III}(Me_2L)]^{+} + 2H^{+} + e^{-} \quad (66)$$

As the pH is increased above 4.1, the $\Delta E_{1/2}$/pH unit slope decreases as $[Fe^{II}(Me_2LH)]^{+}$ becomes more prevalent in solution. Between the pHs of 5.6 and 6.6, a reversible one-electron/one-proton pH-dependent couple (60 mV/pH unit) is observed corresponding to Eq. (67):

$$[Fe^{II}(Me_2LH)]^{+} \rightleftharpoons [Fe^{III}(Me_2L)]^{+} + H^{+} + e^{-} \quad (67)$$

For pH > 8.2, a reversible one-electron pH-independent couple is observed [Eq. (68)]:

$$[Fe^{II}(Me_2L)] \rightleftharpoons [Fe^{III}(Me_2L)]^{+} + e^{-} \quad (68)$$

Analogous results are obtained for the bis(tridentate oxime) complex $[Fe^{II}(dpeH)_2]^{2+}$ [dpeH is 2-(2-pyridylethyl) imimo-3-butanone oxime] with pK_as of 4.37 and 6.38 [74]. The PCET behavior is summarized in Eqs. (69)–(71). In the pH range 1 to 4, a pseudo-reversible one-electron/two-proton pH-dependent couple (120 mV/pH unit) is observed:

$$[Fe^{II}(dpeH)_2]^{2+} \rightleftharpoons [Fe^{III}(dpe)_2]^{+} + 2H^{+} + e^{-} \quad (69)$$

At intermediate pHs (4.5 to 6.5), the Fe(II) complex is deprotonated, and the pseudo-reversible one-electron/one-proton pH-dependent ($\Delta E_{1/2} = 60$ mV/pH unit) couple is observed:

$$[Fe^{II}(dpeH)(DPE)]^{+} \rightleftharpoons [Fe^{III}(dpe)_2]^{+} + H^{+} + e^{-} \quad (70)$$

At pH > 7, the iron(II) complex is fully deprotonated and the reversible one-electron Fe(III/II) couple is pH-independent:

$$[Fe^{II}(dpe)_2] \rightleftharpoons [Fe^{III}(dpe)_2]^{+} + e^{-} \quad (71)$$

Similar PCET behavior was observed for the analogous iron(II) dpmH oxime complex [dpmH is 2-(2-pyridylmethyl) imimo-3-butanone oxime] [74]. Based on the pH–potential diagram, the following redox processes can be inferred.

pH 2 to 4:

$$[Fe^{II}(dpmH)_2]^{2+} \rightleftharpoons [Fe^{III}(dpm)_2]^{+} + 2H^{+} + e^{-} \quad (72)$$

pH 4 to 7:

$$[Fe^{II}(dpmH)(dpm)]^{+} \rightleftharpoons [Fe^{III}(dpm)_2]^{+} + H^{+} + e^{-} \quad (73)$$

pH 7 to 10:

$$[Fe^{II}(dpm)_2] \rightleftharpoons [Fe^{III}(dpm)_2]^{+} + e^{-} \quad (74)$$

In the original paper, however, the one-electron/one-proton couple [Eq. (73)] was assigned for the pH range 2 to 7, possibly because the isolated complex contains one protonated oxime and one deprotonated ($pK^{II}_{a,2} = 6.82$, consistent with the

change from a one-electron/one-proton couple to a pH-independent couple at pH 7) [74]. The PCET reactions in Eqs. (72)–(74) appear to be a better fit to the pH–potential diagram, and change from a one-electron/two-proton couple to a one-electron/one-proton couple at pH 4 would give $pK^{II}_{a,1} \approx 4$, which is consistent with the $pK_{a,1}$ value measured for the analogous $[Fe^{II}(dpeH)_2]^{2+}$ complex.

Cyclic voltammetry of bis(dimethylglyoxime)copper(II), $Cu^{II}(dmgH)_2$, has also been reported to exhibit a Cu(III/II) couple which varies with pH by 59 mV/pH unit in the range pH 4.1 to 8.5 [75]. The oxime hydrogens in bis(glyoxime) complexes are not expected to be very acidic due to strong hydrogen bonding to the other oxime group [76]; therefore, it is not clear if the pH dependence arises from deprotonation of an oxime group, or deprotonation of an axial H_2O, which coordinates in aqueous solution.

3. Concluding remarks

The complexes described above do not constitute a comprehensive list of metal-localized pH-dependent redox couples. Isolated examples of complexes showing pH-dependent electrochemistry were not included, nor were complexes exhibiting pH-dependent redox couples based on changes in conformation and/or coordination number. Rather, families of complexes were chosen to illustrate the principles outlined in the first part of the review. Taken together, the common features of these complexes (rapid, reversible proton and electron transfers, remote ionizable protons which perturb the metal center, potentials and pK_a values within measurable ranges under aqueous conditions) serve as a blueprint for the design of models for proton-coupled electron transfer reactions based on transition metal complexes.

Ligand abbreviations

14TMC	1,4,8,12-tetramethyl-1,4,8,11-tetraazocyclotetradecane
$bibzimH_2$	2,2′-bibenzimidazole
bzimH	benzimidazole
bispicen	*N*,*N*′-bis(2-methylpyridyl)ethane-1,2-diamine
bpy	2,2′-bipyridine
dpeH	2-(2-pyridylethyl) imino-3-butanone oxime
dpmH	2-(2-pyridylmethyl) imino-3-butanone oxime
dmgH	dimethylglyoxime
edda	ethylenediamine-*N*,*N*′-diacetate
edta	ethylenediamine-*N*,*N*,*N*′,*N*′-tetraacetate
imH	imidazole
L′	1,4,7-trimethyl-1,4,7-triazacyclononane
Me_2LH_2	3,14-dimethyl-4,7,10,13-tetra-azahexadeca-3,13-diene-2,15-dione dioxime
Me_2TH	*N*-β-aminoethyl-isonitrosoethyl methyl ketimine

pap	2-(phenylazo)pyridine
phen	1,10-phenanthroline
pic	picolinate
py	pyridine
py(bzimH)$_2$	2,6-bis(benzimidazol-2-yl)pyridine
pytrzH	3-(pyridin-2yl)-1,2,4-triazole
pyz	pyrazine
pzH	pyrazole
sar	sarcophagine
tmen	*N*,*N*,*N*′,*N*′-tetramethylethylenediamine
tpm	tris(1-pyrazolyl)methane
tpy	2,2′:6,2′-terpyridine

References

[1] S.I. Bailey, I.M. Ritchie, F.R. Hewgill, J. Chem. Soc., Perkin Trans. II (1983) 645.
[2] J. March, Advanced Organic Chemistry, Wiley-Interscience, New York, 3rd edn., 1985, Chapter 19.
[3] A.L. Lehninger, Principles of Biochemistry, Worth Publishers, New York, 1982.
[4] G.T. Babcock, P.M. Callahan, Biochemistry 22 (1983) 2314.
[5] G.D. Rydstrom, G.D. Eyntan, E. Eyntan, B. Persson, Chem. Scr. 27B (1987) 83.
[6] K.N. Raymond, Adv. Chem. Ser. 162 (1977) 33.
[7] K.N. Raymond, G. Müller, B.F. Matzanke, Top. Curr. Chem. 123 (1984) 50.
[8] E.I. Stiefel, Proc. Nat. Acad. Sci. USA 70 (1973) 988.
[9] G.W. Brudvig, R.H. Crabtree, Progr. Inorg. Chem. 37 (1989) 99.
[10] R. Manchanda, G.W. Brudvig, R.H. Crabtree, Coord. Chem. Rev. 144 (1995) 1.
[11] M. Pourbaix, Atlas of Electrochemical Equilibria in Aqueous Solution (English transl. J.A. Franklin), Permagon Press, 2nd edn., 1974.
[12] D.G. Brookins, *E*–pH Diagrams for Geochemistry, Springer, New York, 1988.
[13] H.H. Thorp, Chemtracts — Inorg. Chem. 3 (1991) 171.
[14] M.M. Walczak, D.A. Dryer, D.D. Jacobson, M.G. Foss, N.T. Flynn, J. Chem. Ed. 74 (1997) 1195.
[15] N. Sutin, B.S. Brunschwig, Adv. Chem. Ser. 226 (1990) 65.
[16] R.N. Robertson, Protons, Electrons, Phosphorylation and Active Transport, University Press, Cambridge, 1968.
[17] W.A. Pryor, Free Radicals, McGraw-Hill, New York, 1966, Chapter 21.
[18] B.A. Moyer, T.J. Meyer, Inorg. Chem. 20 (1981) 436.
[19] C. Johnson, W. Henderson, R. Shepherd, Inorg. Chem. 23 (1984) 2754 and references cited therein
[20] B. Douglas, D.H. McDaniel, J.J. Alexander, Concepts and Models of Inorganic Chemistry, Wiley, New York, 2nd edn., 1983, Chapter 12.
[21] T. Moeller, J.C. Bailer Jr., J. Kleinberg, C.O. Guss, M.E. Castellion, C. Metz, Chemistry: with Inorganic Qualitative Analysis, Academic Press, Orlando, FL, 2nd edn., 1984.
[22] G. Wulfsberg, Principles of Descriptive Inorganic Chemistry, Brooks/Cole Publishing, CA, 1987, Chapter 2.
[23] J.E. Huheey, Inorganic Chemistry: Principles of Structure and Reactivity, Harper and Row, New York, 3rd edn., 1983, Chapter 7.
[24] W. Stumm, J.J. Morgan, Aquatic Chemistry, Wiley, New York, 2nd edn., 1981, Chapter 7.
[25] A.J. Bard, L.R. Faulkner, Electrochemical Methods: Fundamentals and Applications, Wiley, New York, 1980.
[26] D.H. Evans, K.M. O'Connell, R.A. Petersen, M.J. Kelly, J. Chem. Ed. 60 (1983) 290.
[27] G.A. Mabbott, J. Chem. Ed. 60 (1983) 697.

[28] P.T. Kissinger, W.R. Helneman, J. Chem. Ed. 60 (1983) 702.
[29] J. Osteryoung, J. Chem. Ed. 60 (1983) 296.
[30] J.A. Campbell, R.A. Whitaker, J. Chem. Ed. 46 (1969) 90.
[31] D.W. Barnum, J. Chem. Ed. 59 (1982) 809.
[32] J.C. Angus, B. Lu, M.J. Zappia, J. Appl. Electrochem. 17 (1987) 1.
[33] T.J. Meyer, J. Electrochem. Soc. 131 (1984) 221C.
[34] B.P. Sullivan, D.J. Salmon, T.J. Meyer, J. Peedin, Inorg. Chem. 18 (1979) 3369.
[35] S.V. Ezell, M.S. Thesis, Florida State University, 1993.
[36] S. Goswami, A.R. Chakravorty, A. Chakravorty, Inorg. Chem. 22 (1983) 602.
[37] J. March, Advanced Organic Chemistry: Reactions, Mechanisms, and Structure, Wiley, New York, 3rd edn., 1985, p. 16 and references cited therein.
[38] M.F. Hoq, R. Shepherd, Inorg. Chem. 23 (1984) 1851.
[39] D.D. Perrin, B. Dempsey, Buffers for pH and Metal Ion Control, Wiley, New York, 1974.
[40] A. Bond, M. Haga, Inorg. Chem. 25 (1986) 4507.
[41] P. Ghosh, A. Chakravorty, J. Chem. Soc., Dalton Trans. (1985) 361.
[42] R.C. Engstrom, Anal. Chem. 54 (1982) 2310.
[43] G.E. Cabaniss, A.A. Diamantis, W.R. Murphy Jr.,, R.W. Linton, T.J. Meyer, J. Am. Chem. Soc. 107 (1985) 1845.
[44] M.R. Deakin, K.J. Stutts, R.M. Wightman, J. Electroanal. Chem. 182 (1985) 113.
[45] F. Basolo, R.G. Pearson, Mechanisms of Inorganic Reactions, Wiley, New York, 2nd edn., 1967, p. 31.
[46] K.J. Takeuchi, G.J. Samuels, S.W. Gersten, J.A. Gilbert, T.J. Meyer, Inorg. Chem. 22 (1983) 1407.
[47] J.C. Dobson, T.J. Meyer, Inorg. Chem. 27 (1988) 3283.
[48] B.A. Moyer, T.J. Meyer, J. Am. Chem. Soc. 100 (1978) 3601.
[49] K.J. Takeuchi, M.S. Thompson, D.W. Pipes, T.J. Meyer, Inorg. Chem. 23 (1984) 1845.
[50] C. Ho, C. Che, T. Lay, J. Chem. Soc., Dalton Trans. (1990) 967.
[51] A. Llobet, P. Doppelt, T. Meyer, J. Inorg. Chem. 27 (1988) 514.
[52] M.E. Marmion, K.J. Takeuchi, J. Am. Chem. Soc. 108 (1986) 510.
[53] M.E. Marmion, K.J. Takeuchi, J. Am. Chem. Soc. 110 (1988) 1472.
[54] R.B. Baar, F.C. Anson, J. Electroanal. Chem. 187 (1985) 265.
[55] C. Che, T. Lau, C. Poon, J. Am. Chem. Soc. 112 (1990) 5176.
[56] R. Manchanda, H.H. Thorp, G.W. Brudvig, R.H. Crabtree, Inorg. Chem. 30 (1991) 494.
[57] R. Manchanda, H.H. Thorp, G.W. Brudvig, R.H. Crabtree, Inorg. Chem. 31 (1992) 4040.
[58] R. Hage, B. Krijnen, J.B. Warnaar, F. Hartl, D.J. Stufkens, T.L. Snoeck, Inorg. Chem. 34 (1995) 4973.
[59] J.A. Gilbert, D.S. Eggleston, W.R. Murphy Jr.,, D.A. Geselowsitz, S.W. Gersten, D.J. Hodgson, T.J. Meyer, J. Am. Chem. Soc. 107 (1985) 3855.
[60] M. Goto, M. Takeshita, N. Kanda, T. Sakai, V.L. Goedken, Inorg. Chem. 24 (1985) 582.
[61] K.-F. Chin, K.-Y. Wong, C.-M. Che, J. Chem. Soc., Dalton Trans. (1993) 197.
[62] K.-Y. Wong, C.-M. Che, C.-K. Li, W.-H. Chiu, Z.-Y. Zhou, T.C.W. Mak, J. Chem. Soc., Chem Commun. (1992) 754.
[63] P. Bernhard, F.C. Anson, Inorg. Chem. 28 (1989) 3273.
[64] B.E. Buchanan, R. Wang, J.G. Vos, R. Hage, J.G. Haasnoot, J. Reeddijk, Inorg. Chem. 29 (1990) 3263.
[65] J.G. Vos, J.G. Haasnoot, G. Vos, Inorg. Chim. Acta 71 (1983) 155.
[66] R. Hage, R. Prins, J.G. Haasnoot, J. Reedijk, J.G. Vos, J. Chem. Soc., Dalton Trans. (1987) 1389.
[67] B.P. Sullivan, D.J. Salmon, T.J. Meyer, J. Peedin, Inorg. Chem. 18 (1979) 3369–3374.
[68] X. Xiaoming, M. Haga, T. Matsumura-Inoue, Y. Ru, A.W. Addison, K. Kano, J. Chem. Soc., Dalton Trans. (1993) 2477.
[69] J.K. Blaho, Ph.D. Dissertation, Florida State University, 1993.
[70] J.G. Mohanty, A. Chakravorty, Inorg. Chem. 15 (1976) 2912.
[71] J.G. Mohanty, R.P. Singh, A.N. Singh, A. Chakravorty, J. Indian Chem. Soc. LIV (1977) 219.

[72] A.N. Singh, R.P. Singh, J.G. Mohanty, A. Chakravorty, Inorg. Chem. 16 (1977) 2597.
[73] J.G. Mohanty, A. Chakravorty, Inorg. Chem. 16 (1977) 1561.
[74] N.M. Levy, M.C. Laranjeira, A. Neves, C.V. Franco, J. Coord. Chem. 38 (1996) 259.
[75] Y. Sulfab, Polyhedron 8 (1989) 2409.
[76] F.A. Cotton, G. Wilkinson, Advanced Inorganic Chemistry, Wiley, New York, 5th edn., 1988, p. 366.